Diffusion-Limited Rates for Monoclonal Antibody Binding to Cytochrome *c*†

C. S. Raman,‡ Ronald Jemmerson,§ Barry T. Nall,*,‡ and Michael J. Allen‡

Department of Biochemistry, University of Texas Health Science Center, San Antonio, Texas 78284-7760, and Department of Microbiology, University of Minnesota, Minneapolis, Minnesota 55455-0312

Received March 6, 1992; Revised Manuscript Received August 4, 1992

ABSTRACT: The kinetic and spectroscopic changes accompanying the binding of two monoclonal antibodies to the oxidized form of horse heart cytochrome *c* have been investigated. The two epitopes recognized by the antibodies are distinct and noninteracting: antibody 2B5 binds to native cytochrome *c* near a type II turn (residue 44) while antibody 5F8 binds on the opposite face of the protein near the amino terminus of an α-helical segment (residue 60). Antibody–cytochrome *c* binding obeys a simple bimolecular reaction mechanism with second-order rate constants approaching those expected for diffusion-limited protein–protein interactions. The association rate constants have small activation enthalpies and are inversely dependent on solvent viscosity, as expected for diffusion-controlled reactions. There is a moderate ionic strength dependence of the rate of association between the 2B5 antibody and cytochrome *c*, with the rate constant increasing about 4-fold as the ionic strength is varied between 0.14 and 0 M. Comparison of the rates for antibody–cytochrome *c* complex formation for binding to the reduced-native, oxidized-native, and alkaline conformations shows that for MAb 2B5 the forward rate constant depends slightly on cytochrome *c* conformation. Investigation of the pH-induced transition between the native and alkaline conformational states for free cytochrome *c* and for antibody–cytochrome *c* complexes shows that antibody binding stabilizes the native form of the protein. The rate of the native to alkaline conformational change is decreased for cytochrome *c* in complex with antibody 2B5 but is unchanged in complexes with antibody 5F8, suggesting a structural change in the epitope near residue 44 but no change in the epitope near residue 60 between the alkaline conformation and the alkaline–native transition state. A combination of electronic absorption, fluorescence, circular dichroism, and magnetic circular dichroism spectroscopies has been used to probe the geometric and electronic structure of the heme in free cytochrome *c* and antibody-complexed cytochrome *c*. Antibody binding to cytochrome *c* causes no change in the magnetic circular dichroism spectrum, suggesting that the coordination sphere of the metal ion remains unchanged. Changes in heme absorption and circular dichroism spectra accompanying binding of the 2B5 antibody to cytochrome *c* show that binding alters the heme environment, possibly by inducing a structural change within the protein antigen. This antibody is known to bind in the vicinity of the heme crevice. The antibody 5F8 which binds on the opposite surface does not elicit these effects.

Antibodies play an important biological role in the recognition of foreign antigens and are useful tools for detection, characterization, and quantitation of proteins and protein conformational states. Thus, it is important to have a detailed mechanistic understanding of association reactions between antibodies and antigens. While the kinetic mechanism of antibody binding to small-molecule antigens has been characterized in some detail, the potentially more interesting problem of antibody binding to epitopes on protein antigens has received less attention. With the exception of a few pioneering studies (Friguet et al., 1989; Noble et al., 1969), there is very little information on the kinetic properties of antibody–protein antigen binding reactions. In particular, mechanistic studies of binding are few for systems simple enough and sensitive enough to detect intermediates in antibody–protein antigen reactions. In the present study, the use of monoclonal rather than polyclonal antibodies (Noble et al., 1969) reduces the minimal kinetic mechanism to that of a simple biomolecular reaction. Any deviations from the simple mechanism (Friguet et al., 1989) provide direct evidence of intermediate states of the reacting species.

Our model system for studying the kinetics of antibody–protein antigen binding makes use of horse cytochrome *c* as the protein antigen. Cytochrome *c* contains a covalently bound heme which is an efficient quencher of tryptophan fluorescence. Antibodies have one or more tryptophan residues near the antigen combining site, so fluorescence studies of antibody–cytochrome *c* binding are exquisitely sensitive (Friguet et al., 1989; Noble et al., 1969). Two different monoclonal antibodies have been studied. One antibody (2B5) is known to bind to native cytochrome *c* near a type II turn (residue 44) while the other (5F8) binds to a distinct epitope on the opposite face of the protein near the amino terminus of an α-helical segment (residue 60) (Goshorn et al., 1991). Although some studies of antibody binding to small-molecule antigens indicate kinetic complexity and thus intermediate states (Kranz et al., 1982), the kinetic results reported here are surprisingly simple and are consistent with a two-state diffusion-controlled bimolecular binding mechanism.

A comparison is made of the association rate constants for binding to different conformational states of cytochrome *c*.

‡ Supported by National Institute of General Medical Sciences Grant GM32980 (B.T.N.), Robert A. Welch Foundation Grant AQ838 (B.T.N.), and National Science Foundation Grant DMB-9019181 (R.J.).

* Address correspondence to this author at the Department of Biochemistry, University of Texas Health Science Center, 7703 Floyd Curl Dr., San Antonio, TX 78284-7760.

‡ University of Texas Health Science Center.

§ University of Minnesota.

0006-2960/92/0431-10370$03.00/0

Two of the conformational states studied, the oxidized and reduced native forms, have been shown by X-ray crystallography to have very similar three-dimensional structures (Bushnell et al., 1990; Takano & Dickerson, 1981a,b), but show differences in global and local conformational stability (Feng et al., 1990; Wand et al., 1986), compressibility (Eden et al., 1982), and, perhaps, internal or segmental mobility. Another conformer, the alkaline form, is known to differ from the native protein in heme ligation (Davis et al., 1974; Gupta & Koenig, 1971; Hettinger & Harbury, 1964; Shechter & Saludjian, 1967; Smith & Millett, 1980; Wallace, 1984; Wilgus & Stellwagen, 1974) but retains much of the secondary structure of the native state (Dohne et al., 1989). Comparisons of binding rates yield the result that the rate constants are the same for binding of one MAb[1] to the oxidized or reduced native forms while a second MAb has a slightly smaller rate constant for binding reduced rather than oxidized cytochrome *c*. Similarly, the rate constant for association differs in the alkaline conformation for one epitope, but not the other. The effects of MAb binding on the rate of a protein conformational change have been investigated. The rate of the native to alkaline conformational change is decreased in the presence of one MAb but not the other, suggesting that MAbs may be useful in characterizing transition states for protein conformational changes and folding reactions.

Visible spectroscopy has been used to probe antibody-induced structural changes within the protein antigen. Absorbance and circular dichroism (CD) spectral analysis of one of the antibody–protein complexes shows evidence of a change in the electronic environment of the heme within the complex. The spectroscopic changes prove than antibody binding alters heme environment and suggest the possibility of antibody-induced changes in the conformation of cytochrome *c*.

MATERIALS AND METHODS

Sucrose and glycerol were obtained from Fluka. All other reagents were of analytical grade. For all experiments, the temperature was regulated to within a few tenths of a degree using circulating water baths. Horse heart cytochrome *c* was purchased from Sigma (type VI) and purified chromatographically by the method of Brautigan et al. (1978). To prepare fully oxidized cytochrome *c*, a slight molar excess of potassium ferricyanide was added to a cytochrome *c* stock solution and the ferricyanide removed by G-25 Sephadex chromatography. Reduced cytochrome *c* was prepared by adding β-ME or DTT in molar excess to the protein solution and removing the reducing agent by G-25 Sephadex chromatography. The concentrations of cytochrome *c* and monoclonal antibody were assessed spectrophotometrically using $\epsilon_{410} = 106\,100\ M^{-1}\ cm^{-1}$ (Margoliash & Frohwirt, 1959) and $\epsilon_{280} = 210\,000\ M^{-1}\ cm^{-1}$ (Corradin et al., 1984), respectively (assuming an MAb molecular weight of 150 000).

Monoclonal Antibody Purification. Hybridoma cells were grown to high density in roller bottles using DMEM (Hyclone)/10% FBS (Whittaker Biosciences) media. Cells were removed by centrifugation at 5000 rpm, 4 °C, for 20 min, followed by filtration of the supernatent through a 0.45-μm filter (Amicon). Antibody was concentrated and purified by affinity chromatography as follows: horse cytochrome *c* (Sigma, type VI) coupled Affi-gel 10 resin (Bio-Rad) was added to the antibody-containing supernatant and rolled in roller bottles overnight at 4 °C. The resin was removed from the supernatant by filtration and extensively washed with 0.1 M sodium phosphate, 0.05% Tween-20, and 0.15 M NaCl, pH 7.0, followed by 0.1 M sodium phosphate, 0.05% Tween-20, and 1 M NaCl, pH 7.0, and finally with 0.1 M sodium phosphate, pH 7.0. Antibody was eluted from the resin using 0.1 M glycine, 0.4 M Gdn·HCl, pH 2.9. Fractions were neutralized by the addition of 1 M Tris. Antibody was dialyzed extensively with 0.1 M sodium phosphate, pH 7.0, and checked for purity using SDS–PAGE. Antibodies 2B5 and 5F8 were isotyped using a mouse typer kit from Bio-Rad and found to be IgG_{2a}:κ and IgG_1:κ, respectively. Pure antibody solutions were stored at −20 °C in 30% glycerol. Prior to use, glycerol was removed by gel filtration on a Sephadex G-25 column equilibrated with 0.1 M sodium phosphate buffer, pH 7.0.

Absorption, Circular Dichroism, and Magnetic Circular Dichroism Spectra. All spectroscopic measurements were carried out at 20 °C with the exception of MCD spectra which were obtained at ambient temperature. Visible absorption spectra were recorded with either a Shimadzu UV-260 or an HP 8452A diode array spectrophotometer. CD and MCD spectra were collected with a Jasco J-500C spectropolarimeter equipped with a Jasco MCD-1B electromagnet, which produces a longitudinal magnetic field of 1.5 T. The magnetic field was determined using a Gauss meter. MCD spectra were corrected for the natural CD component. The instrument was calibrated with (+)-10-camphorsulfonic acid. Data were collected at 0.2-nm intervals with a scan rate of 5 nm min^{-1}, a spectral band width of 1 nm, and an instrumental time constant of 4 s; The scanning window (product of the time constant and scan rate) was ≤0.33 nm (Hennessey & Johnson, 1982).

The path length of the cell was 1 cm, and the absorbance of the sample over the CD range was always maintained below 1.0 absorbance unit. All CD experiments employed a slight excess of MAb sites to eliminate free cytochrome *c* in solution. CD spectra are reported in terms of differential molar absorption coefficients, $\Delta\epsilon = \epsilon_L - \epsilon_R$, in $M^{-1}\ cm^{-1}$ (the molar ellipticity, [θ], given in deg $cm^2\ dmol^{-1}$, equals $3300\Delta\epsilon$). All CD spectra represent the average of two scans.

Kinetic Measurements. The kinetics of association between the antibodies and cytochrome *c* were studied using a three-syringe Biologic SFM-3 stopped-flow spectrophotometer (Molecular Kinetics, Pullman, WA) or an SLM 500C spectrofluorometer (SLM Instruments, Urbana, IL) with a thermostatically controlled cuvette holder maintained at 20 °C. The mixing dead time for the stopped-flow instrument is about 2.5 ms while the (manual) mixing time in the spectrofluorometer is about 5 s. The fluorometer excitation and emission wavelengths were 285 and 350 nm with the slits set to give a band-pass of 5 and 7.5 nm, respectively. For the stopped-flow experiments, the excitation was at 285 nm with the fluorescence emission observed through a 350-nm band-pass filter.

For stopped-flow measurements, syringe 1 contained 0.1 M sodium phosphate, pH 7.0, syringe 2 contained MAb in the same buffer, and syringe 3 contained cytochrome *c* at pH 7.0 or pH 10.0. Final concentrations of cytochrome *c* and MAb in the observation cuvette (2-mm path length, 40-μL volume) were varied by injecting different volumes from the drive syringes (final pH 7.0). In all cases, the time course of complex

[1] Abbreviations: MAb, monoclonal antibody; CD, circular dichroism; MCD, magnetic circular dichroism; DTT, dithiothreitol; SDS, sodium dodecyl sulfate; β-ME, β-mercaptoethanol; Gdn·HCl, guanidine hydrochloride; SDS–PAGE, polyacrylamide gel electrophoresis in the presence of sodium dodecyl sulfate; T, telsa (=10 000 G); DMEM, Dulbecco's modified Eagle's media; FBS, fetal bovine serum; NMR, nuclear magnetic resonance.

formation was monitored by fluorescence quenching of the MAb on binding cytochrome *c*. The quenching arises from the heme of cytochrome *c* which quenches the fluorescence from tryptophan side chains of the MAb in the vicinity of the antigen binding site (Noble et al., 1969). The fluorescence at 350 nm was measured through a 350-nm band-pass filter at a right angle to the incident light (excitation at 285 nm). Bimolecular rate constants (k_1) were calculated by using the Enzfitter program (Elsevier-Biosoft) to fit the kinetic data to the equation:

$$F(t) = F_0 + (F_\infty - F_0)\{(1 - \exp[(a_t - c_t)k_1 t])/(1 - (a_t/c_t)\exp[(a_t - c_t)k_1 t])\}$$

for $c_t > a_t$ or

$$F(t) = F_0 + (F_\infty - F_0)(a_t/c_t)\{(1 - \exp[(a_t - c_t)k_1 t])/(1 - (a_t/c_t)\exp[(a_t - c_t)k_1 t])\}$$

for $a_t > c_t$ where a_t and c_t are the total concentration of antibody binding sites and the total concentration of cytochrome *c*, respectively. $F(t)$, F_0, and F_∞ are, respectively, the fluorescence signals at time t, time $t = 0$, and after completion of the reaction.

The rate of the alkaline conformational change was determined by mixing equal volumes of cytochrome *c* initially at pH 10 with 0.1 M sodium phosphate, pH 7.0. The reaction was monitored at 418 nm in a 1-cm cuvette at 20 °C. Apparent first-order rate constants (k_{obs}) were obtained by least-squares fits of the absorbance data to the equation:

$$A_\infty - A(t) = (A_\infty - A_0)\exp(-k_{obs}t)$$

where A_0 is the absorbance at $t = 0$, A_∞ the final absorbance on completion of the reaction, and $A(t)$ the absorbance at time t.

The effects of ionic strength, temperature, and viscosity on the association rate were all studied under pseudo-first-order conditions with cytochrome *c* in a 10-fold excess over the antibody sites. Quenching studies were initiated by mixing 0.1 mL of a cytochrome *c* solution with 2.9 mL of antibody-containing buffer so that the final concentrations after mixing were 1×10^{-7} M cytochrome *c* and 1×10^{-8} M antibody (binding sites). All rate constants presented are the average of three independent measurements. At low temperatures, condensation on the optical components of the fluorometer was prevented by flushing the cell chamber with dry nitrogen gas. The fluorescence data were processed using a data file format conversion program (written by Sudha Veeraraghavan) and analyzed by nonlinear least-squares regression using the program BioKine (Molecular Kinetics, Pullman, WA). Pseudo-first-order rate constants (k_{obs}) were obtained by least-squares fits of the fluorescence data to the equation:

$$F(t) - F_\infty = (F_0 - F_\infty)\exp(-k_{obs}t)$$

where F_0 is the fluorescence at $t = 0$, F_∞ the final fluorescence on completion of the reaction, and $F(t)$ the fluorescence at time t. The pseudo-first-order rate constants were used to calculate the biomolecular association rate constant: $k_1 = k_{obs}/[\text{cytochrome } c]$.

Activation parameters were obtained from the temperature dependence of the association rate constant, k_1, using the Eyring equation:

$$\Delta G^\ddagger/T = R \ln [(k_b T/h)(1/k_1)]$$

where $R = 1.987$ cal K^{-1} mol^{-1}, $k_b = 1.38 \times 10^{-16}$ erg K^{-1}, $h = 6.626 \times 10^{-27}$ erg s, and T is temperature in degrees kelvin. Since $\Delta G^\ddagger/T = \Delta H^\ddagger(1/T) - \Delta S^\ddagger$, a plot of $\Delta G^\ddagger/T$ versus $1/T$ yields the activation parameters. Units of liters per mole per second have been used for the bimolecular association rate constant, k_1.

Dissociation rate constants were measured by an ELISA procedure in which the antibody–cytochrome *c* complex was incubated in the wells of a microtiter plate coated with cytochrome *c*. The complex was preformed by mixing equal volumes of cytochrome *c* (4 nM) and antibody (2 nM) in 0.5% (w/v) BSA/0.02% (w/v) sodium azide in 0.1 M sodium phosphate. The horse cytochrome *c* was adsorbed to the wells of the 96-well ELISA plate by adding 150 μL of 1 μM cytochrome *c* in 0.1 M sodium phosphate, pH 7, to each well and incubating at 4 °C overnight. Unreacted sites on the ELISA wells were blocked by adding 300 μL of the above 0.5% BSA buffer to each well and incubating for 30 min at room temperature. One hundred fifty microliters of the cytochrome *c*–antibody complex was added to triplicate wells and incubated at room temperature. A control of antibody alone in 0.5% BSA buffer was included in the triplicate wells. After 1-h incubation, one row of wells containing the cytochrome *c*–antibody complex and the antibody control solutions was aspirated, rinsed with buffer (50 mM Tris, 0.2 M NaCl, and 0.05% Tween-20, pH 7.2), and refilled with 200 μL of 0.5% BSA buffer. This was repeated for the remaining rows of solutions after 3, 6, 9, 12, 25, and 29 h. A VECTASTAIN (VECTOR Laboratories) alkaline phosphatase ABC kit was used to develop the ELISA plate according to the manufacturer's instructions. The absorbance of the ELISA wells was recorded at 405 nm. Assuming that the dissociation rate is equal to the rate at which antibody binds to the wells, the dissociation rate constant was obtained by fitting the antibody binding data to a single-exponential decay process. The dissociation rate measurements were repeated using 0.1 μM cytochrome *c* to coat the wells with similar results, showing that the off rates are independent of the concentration of antigen used to coat the wells. It should be emphasized that the off-rate measurements reported here depend entirely on the assumption that the binding of dissociated antibody to the wells is faster than reassociation of the soluble complex. This is difficult to test directly. Nevertheless, off-rate measurements for the 2B5 antibody–cytochrome *c* complex using biospecific interaction analysis detected by surface plasmon resonance (Pharmacia–BIAcore) give results in agreement with those reported here (M. J. Allen and C. S. Raman, unpublished results). Equilibrium association constants for antibody–cytochrome *c* binding were obtained from the equation $K_a = k_1/k_{-1}$ in which K_a is the equilibrium association constant, k_1 the bimolecular association rate constant, k_{-1} the dissociation rate constant. Use of this relationship for estimating K_a assumes that the binding reaction is a simple two-state process.

Measurement of the Viscosity Dependence of Binding. The viscosity dependence of the 2B5 antibody–cytochrome *c* association rate constant was followed in the presence of gycerol and sucrose. Buffers containing sucrose or glycerol (0–32% w/w) were prepared by dissolving the required amount of the viscous agent in 0.1 M sodium phosphate buffer, pH 7.0. The resulting solutions were filtered through a 0.45-μm membrane to remove suspended particles. The pH readings of viscous mixtures obtained from a glass electrode calibrated with standard buffers were corrected for changes in the junction potential (Gelsema et al., 1977). The relative viscosity values were obtained (Weast, 1984) and confirmed by measurements using a Cannon–Ubbelohde viscometer at 20 °C. In order to

eliminate schlieren effects arising from mixing solutions of varying viscosity, both antibody and cytochrome *c* solutions were prepared in the buffer containing the appropriate concentration of the viscous additive.

Measurement of the Ionic Strength Dependence of Rates. The ionic strength dependence of antibody–cytochrome *c* binding was investigated by varying NaCl concentrations at a fixed concentration (0.007 M) of sodium phosphate. The ionic strength of the solutions was calculated as $I = 0.5\Sigma_i m_i z_i^2$ where m_i are the molarities and z_i the charges of each of the *i* species.

Determination of pK_{app} for the Alkaline Conformational Change. Two stock solutions of oxidized horse cytochrome *c* (4 μM) were prepared, and the pH was adjusted to pH 7.0 and 11.5. To generate different final pH points, various ratios of these two stocks were mixed. The pH of the resulting mixtures was recorded and the absorbance at 418 nm determined using a Hewlett-Packard 8452A diode array spectrophotometer. For determination of the pK_{app} for the alkaline conformational change in the presence of MAb, stock solutions were prepared and analyzed as above except each solution also contained antibody (2.5×10^{-6} M for 2B5 and 2.0×10^{-6} M for 5F8). To determine the pH range over which the complex remains intact, fluorescence emission spectra of the MAb–cytochrome *c* complex were measured as a function of pH. pK_{app} values were calculated by using the Enzfitter program to obtain nonlinear least-squares fits to the equation:

$$A = [A_H + A_L 10^{-n(pH-pK_{app})}]/[1 + 10^{-n(pH-pK_{app})}]$$

where *A* is the absorbance of the alkaline and native forms, A_H is the absorbance of the alkaline form, A_L is the absorbance of the native protein, and *n* is the number of protons involved in the transition. pH and pK_{app} have the usual definitions as the negative logarithms of the hydrogen ion concentration and the proton dissociation constant, respectively.

Isoelectric Focusing of Monoclonal Antibodies. Polyacrylamide isoelectric focusing gels in the pH range 4–8 were cast in 13 × 3 mm tubes (Bio-Rad Model 150A) (Robertson et al., 1987). Calibration of the p*I* was performed using standards obtained from Bio-Rad. Samples containing 20 μg of antibody were applied to the gels. After being focused the pH gradient was measured, and the gels were fixed and stained with Coomassie Brillant Blue R-250.

RESULTS

Spectroscopic Characterization of the Monoclonal Antibody–Cytochrome c Complex. The antibody–cytochrome *c* complex has been characterized by visible spectroscopy, fluorescence, circular dichroism, and magnetic circular dichroism. Visible absorption spectroscopy (Figure 1) shows that the interaction between the 2B5 antibody and oxidized cytochrome *c* results in a 2-nm red shift in the spectrum in the Soret region (from 410 nm to 412 nm) and a positive difference absorption spectrum with a maximum extinction change of about 7500 M^{-1} cm^{-1} at 412 nm. In contrast, there are no significant changes in the Soret region of the spectrum of cytochrome *c* on complex formation with the 5F8 antibody.

Fluorescence titrations of the 2B5 antibody (Figure 2A) and the 5F8 antibody (Figure 2B) with cytochrome *c* show that the stoichiometry of binding is about two molecules of cytochrome *c* to one antibody molecule. Small deviations from the expected two to one binding stoichiometry are probably because the same (approximate) molar extinction

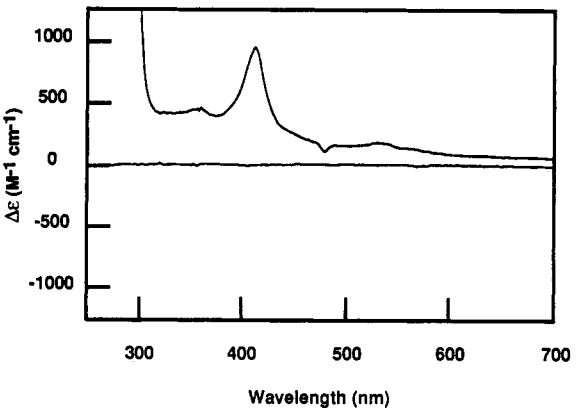

FIGURE 1: Soret difference absorption spectrum generated by the interaction of the 2B5 antibody with cytochrome *c* in 0.1 M sodium phosphate, pH 7.0. Cytochrome *c* and 2B5 antibody binding sites were both present at a concentration of 4×10^{-6} M corresponding to a 1:1 complex. Δε is the change in extinction coefficient per mole of heme.

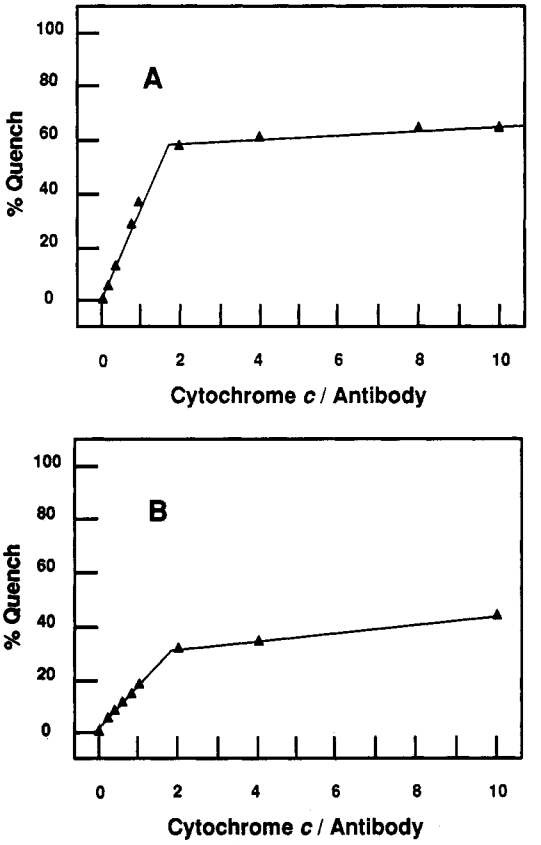

FIGURE 2: Fluorescence quenching of the 2B5 antibody (A) and the 5F8 antibody (B) on titration with cytochrome *c*. For each cytochrome *c* concentration, quenching of the antibody fluorescence is calculated as percent quench = 100 $(1 - F/F^0)$, where *F* is the fluorescence emission of the solution containing antibody and cytochrome *c* and F^0 is the fluorescence emission of the solution containing only antibody. Antibody concentrations are kept constant at 1.0×10^{-7} M for the 2B5 antibody and 5×10^{-7} M for the 5F8 antibody. Excitation is at 285 nm. Other conditions are 20 °C, 0.1 M sodium phosphate buffer, pH 7.

coefficient was used for both antibodies. It seems likely that the antibodies differ slightly in their aromatic amino acid composition and have small differences in extinction coefficient. On binding cytochrome *c*, there is a small but significant blue shift in the maximum of the fluorescence emission spectrum of the 2B5 antibody from 348 nm to 345 nm, but no significant change in the emission maximum for the 5F8 antibody.

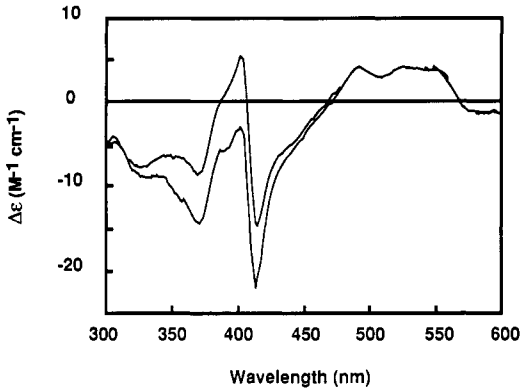

FIGURE 3: Soret circular dichroism spectra of free cytochrome *c* and cytochrome *c* in complex with the 2B5 antibody. The upper trace is that of the free cytochrome *c* while the lower trace is for the antibody–cytochrome *c* complex. Conditions are 0.1 M sodium phosphate, pH 7.0, at 20 °C. Cytochrome *c* concentration was 9.8 × 10^{-6} M, and the antibody binding sites concentration was 10.1 × 10^{-6} M.

Figure 3 shows that binding of the 2B5 antibody to cytochrome *c* induces large changes in the intensity of the visible CD spectrum, especially between 350 and 450 nm. There are no significant changes in the visible CD spectrum when the 5F8 antibody binds cytochrome *c* (data not shown). Magnetic circular dichroism (MCD) spectra have also been obtained for the 2B5 antibody–cytochrome *c* complex, but the visible MCD spectrum shows only minor changes on complex formation.

Biomolecular Association Rate Constants. To verify that the antibody–cytochrome *c* binding process follows a bimolecular rate law, the observed bimolecular rate constants have been measured as a function of MAb and cytochrome *c* concentration (e.g., Figure 4 for MAb 5F8 binding to oxidized cytochrome *c*). Optical spectroscopy indicates that the heme environment changes for cytochrome *c* bound by the 2B5 antibody, suggesting the possibility of an induced structural change in the antigen. In an attempt to detect kinetic intermediates associated with a possible 2B5 MAb-induced structural change, the test of the bimolecular rate law has been extended over a wide cytochrome *c* concentration range. The results (not shown) show that the 2B5 MAb–oxidized cytochrome *c* binding reaction remains consistent with a bimolecular reaction mechanism over a 300-fold cytochrome *c* concentration range (from 7.5 × 10^{-7} to 2.4 × 10^{-4} M). For both MAb 2B5 and MAb 5F8, measurements similar to those in Figure 4 have been carried out for binding to oxidized, reduced, and alkaline cytochrome *c* over a range of MAb and cytochrome *c* concentrations (data not shown). All of the reactions obey a biomolecular rate law and have the association rate constants listed in Table I.

Temperature Dependence of Association Rate Constants. The temperature dependence of the biomolecular rate constant for the 2B5 antibody–cytochrome *c* association reaction has been measured. From the Eyring plot (Figure 5), thermodynamic reaction rate parameters of $\Delta H^{\ddagger}$ = 5.5 ± 0.1 kcal mol^{-1} and $\Delta S^{\ddagger}$ = −12.8 ± 0.4 cal K^{-1} mol^{-1} are obtained. Therefore, at T = 298 K, there is an activation free energy barrier of $\Delta G^{\ddagger}$ = 9.3 kcal mol^{-1} of which the entropic contribution is $-T\Delta S^{\ddagger}$ = 3.8 kcal mol^{-1}. A similar Eyring plot for data obtained with the 5F8 antibody (data not shown) yields the following parameters: $\Delta H^{\ddagger}$ = 3.8 ± 0.8 kcal mol^{-1} and $\Delta S^{\ddagger}$ = −17.6 ± 2.7 cal K^{-1} mol^{-1}. In this case, $\Delta G^{\ddagger}$ = 9.0 kcal mol^{-1} at T = 298 K, and the entropic contribution is $-T\Delta S^{\ddagger}$ = 5.2 kcal mol^{-1}. The Eyring plots show less scatter

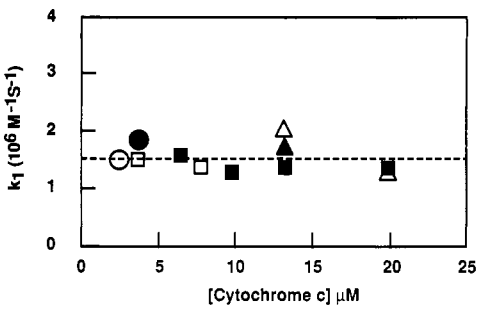

FIGURE 4: Test of the bimolecular rate law for binding of MAb 5F8 to oxidized cytochrome *c*. Apparent bimolecular association rate constants (k_1) are given as a function of cytochrome *c* concentration for binding to the oxidized form of the protein. The dashed line indicates that average value for all the kinetic experiments (see Table I) which is k_1 = (1.5 ± 0.2) × 10^6 M^{-1} s^{-1}. Reactions are initiated by stopped-flow mixing at 20 °C, 0.1 M sodium phosphate, pH 7.0, and binding was monitored by the fluorescence at 350 nm with excitation at 285 nm. Final MAb concentrations are indicated by the symbols: open squares, 1.2 × 10^{-6} M; filled squares, 1.3 × 10^{-6} M; open circles, 1.4 × 10^{-6} M; filled circles, 1.6 × 10^{-6} M; open triangles 2.7 × 10^{-6} M; filled triangles, 4.0 × 10^{-6} M.

for MAb 2B5 than for MAb 5F8. This is probably because the signal changes are larger for MAb 2B5 than for MAb 5F8 on forming a complex with cytochrome *c* (compare Figure 2A,B).

Viscosity Dependence of Binding Rate Constants. Figure 6 presents results of measurements of the viscosity dependence of the 2B5 antibody–cytochrome *c* association reaction. The bimolecular association rate constant is found to be inversely proportional to the relative viscosity of the solvent when either sucrose or glycerol are used as additives. The dependence on viscosity is very similar for glycerol versus sucrose, although the rate constant is slightly, but significantly, less sensitive to solvent viscosity when glycerol is used as the viscous additive. For example, a plot of the inverse of the rate constant versus the relative viscosity of the solvent has a slope of 1.06 when sucrose is the viscous additive but is reduced to 0.8 in the presence of glycerol. Similar data for antibody 5F8 using sucrose as the viscous additive yield a slope of 1.2 for the plot of the inverse of the rate constant versus relative viscosity (data not shown). The data show less scatter for MAb 2B5, probably because of the larger signal change on complex formation.

Ionic Strength Dependence of Binding Rate Constants. Figure 7 gives the ionic strength dependence of the bimolecular rate constant for binding of the 2B5 antibody to cytochrome *c* (measured at 5.6 °C). For binding to oxidized or reduced cytochrome *c*, the rate constant increases in magnitude by a factor of about 4 as the ionic strength is decreased from 0.14 to 0. At 0 ionic strength, the extrapolated rate constants are 1.6 × 10^6 and 1.4 × 10^6 M^{-1} s^{-1} for oxidized and reduced cytochrome *c*, respectively.

To estimate the approximate charge on the monoclonal antibodies, isoelectric focusing experiments were carried out. Isoelectric focusing of both 5F8 and 2B5 MAbs yielded a family of bands within a span of 0.4 pH unit located between pH 5.95 and pH 6.42. This is good agreement with the values reported for MAbs in general (Hamilton et al., 1987). The antibodies used in this work will have a net negative charge at pH 7.0, suggesting that the rates for binding to the positively charged antigen, cytochrome *c*, are likely to be enhanced at low ionic strength. The observed increase in the rate constant on lowering the ionic strength is qualitatively consistent with opposite electrostatic charges on the two macromolecular species.

Table I: Rate and Equilibrium Constants

monoclonal antibody	cytochrome c conformation: oxidized k_1[a] (M^{-1} s^{-1})	oxidized k_{-1}[b] (s^{-1})	oxidized K_a[c] (M^{-1})	reduced k_1[a] (M^{-1} s^{-1})	alkaline k_1[a] (M^{-1} s^{-1})
2B5	$(6.5 \pm 1.0) \times 10^5$	$\sim 8 \times 10^{-5}$	$\sim 9 \times 10^9$	$(5.2 \pm 0.5) \times 10^5$	$(4.2 \pm 0.5) \times 10^5$
5F8	$(1.5 \pm 0.2) \times 10^6$	$(1.0 \pm 0.6) \times 10^{-4}$	1.5×10^{10}	$(1.5 \pm 0.4) \times 10^6$	$(1.5 \pm 0.3) \times 10^6$

[a] Averages of bimolecular association rate constants for binding to different conformations of cytochrome c. For the 2B5 MAb, 33 values are averaged for oxidized cytochrome c, 12 values are averaged for reduced cytochrome c, and 15 values are averaged for binding to alkaline cytochrome c. For 5F8 MAb, 46 values are averaged for oxidized cytochrome c, 14 values are averaged for reduced cytochrome c, and 24 values are averaged for binding to alkaline cytochrome c. Measurements are made at 20 °C. Errors are standard deviations of separate measurements of the association rate constants. [b] The dissociation rate constants were measured using an ELISA procedure (see Materials and Methods). These were carried out at room temperature (~23 °C), 0.1 M sodium phosphate, pH 7.0. For MAb 5F8, the errors in k_{-1} are estimated as the standard deviations of separate measurements. Errors are not given for MAb 2B5 since there were only two successful measurements of the dissociation rate. [c] Equilibrium association constants for monoclonal antibody binding to oxidized cytochrome c have been estimated assuming that $K_a = k_1/k_{-1}$. Note that k_1 was measured at 20 °C while k_{-1} was measured at room temperature (~23 °C).

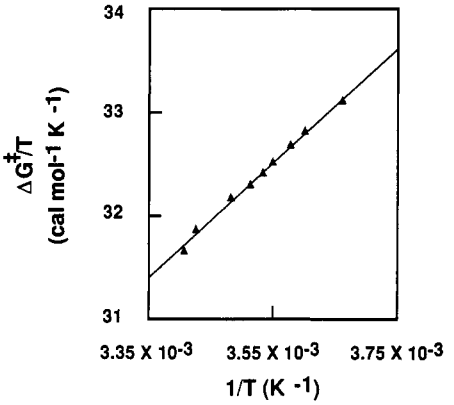

FIGURE 5: Eyring plot of the temperature dependence of the bimolecular association rate constant for the 2B5 antibody. Other conditions are 1×10^{-7} M oxidized cytochrome c, 1×10^{-8} M antibody binding sites, pH 7.0, and 0.1 M sodium phosphate. The values for k_1 are the averages of three separate runs.

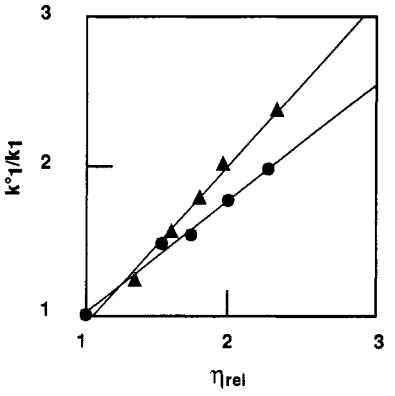

FIGURE 6: Plot of the reciprocal of the relative second-order rate constant for antibody 2B5 binding to oxidized cytochrome c as a function of relative viscosity. The parameters k_1 and k^0_1 are, respectively, the apparent bimolecular rate constants in the presence and absence of the viscous additive. The relative viscosity of the solution is $\eta_{rel} = \eta/\eta_0$ where η is the viscosity in the presence of the viscous additive and η_0 is the viscosity of buffer solution. Filled triangles represent data obtained in the presence of sucrose and filled circles in the presence of glycerol.

Rate of Binding of 2B5 Antibody to the 5F8 Antibody–Cytochrome c Complex. The existence of nonoverlapping epitopes on cytochrome c for the 2B5 antibody and the 5F8 antibody was verified by monitoring the fluorescence quenching on binding 2B5 antibody to a preformed 5F8 antibody–cytochrome c complex. The experiments were carried out at 3.8 °C. The results given in Table II confirm that the epitopes for the two different antibodies are distinct and nonoverlapping.

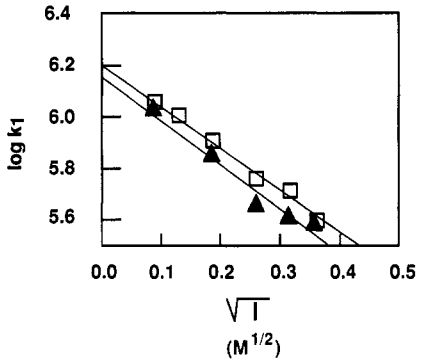

FIGURE 7: Dependence of the bimolecular rate constant for binding of the 2B5 antibody to cytochrome c on the square root of the ionic strength. Open squares are for binding to oxidized cytochrome c and filled triangles are for binding to reduced cytochrome c. Conditions are 0.0074 M sodium phosphate, pH 7.0, and sodium chloride to give the indicated ionic strength. Temperature was regulated at 5.6 °C. Protein concentrations are 1×10^{-7} M oxidized cytochrome c and 1×10^{-8} M antibody binding sites.

Table II: Association Rate Constants for Antibody Binding to a Cytochrome c–Antibody Complex[a]

reaction	association rate constant, k_1 (M^{-1} s^{-1})
2B5 antibody + cytochrome c	$(4.0 \pm 0.3) \times 10^5$
5F8 antibody + cytochrome c	$(6.1 \pm 1) \times 10^5$
2B5 antibody + 5F8 antibody–cytochrome c complex	$(3.3 \pm 0.5) \times 10^5$

[a] The reactions were carried out at 3.8 °C by manual mixing.

Dissociation Rates and Two-State Estimates of Equilibrium Binding Constants. Several unsuccessful attempts were made to measure the equilibrium binding constants for MAb 5F8 and MAb 2B5 binding to cytochrome c. Methods attempted included fluorescence measurements of the extent of complex formation at fixed MAb and variable cytochrome c concentrations and ELISA assays of free antibody in equilibrium with complex (Friguet et al., 1985, 1989; Stevens, 1987). These attempts were successful in demonstrating that the equilibrium association constants exceeded $\sim 10^9$ M^{-1} for both MAb 2B5 and MAb 5F8. We have used an ELISA method (see Materials and Methods) to measure dissociation rate constants. The method involves adsorbed antigen trapping of the antibody released on dissociation from the soluble complex. Five separate measurements of the dissociation rate for the 5F8 MAb–cytochrome c complex gave consistent results for k_{-1} (Table I). For unknown reasons, the results with MAb 2B5 were much less satisfactory. Of four attempts to measure the dissociation rate for the 2B5 MAb–cytochrome c complex, two failed to exhibit kinetics and the other two gave values

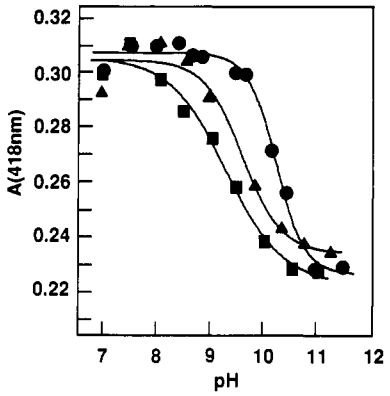

FIGURE 8: Stabilization of native oxidized cytochrome *c* by MAb complex formation. The pH dependence of the absorbance at 418 nm is compared for free oxidized cytochrome *c* (squares), 5F8 MAb–cytochrome *c* complex (triangles), and 2B5 MAb–cytochrome *c* complex (circles). As expected for antibodies raised to native cytochrome *c*, complex formation stabilizes the native conformation of cytochrome *c* relative to the alkaline conformation. The solid lines are theoretical pH titration curves with a "best fit" pK_{app} = 9.3 ± 0.1 for free cytochrome *c*, 9.6 ± 0.2 for the 5F8 MAb–cytochrome *c* complex, and 10.2 ± 0.04 for the 2B5 MAb–cytochrome *c* complex. Measurements are at 20 °C in the presence of 0.1 M sodium phosphate.

Table III: Titration Parameters for pH-Induced Conformational Change in the Presence and Absence of Antibodies[a]

protein species	pK_{app}	*n*
cytochrome *c* (free)	9.3 ± 0.1	0.8 ± 0.2
5F8 MAb–cytochrome *c* complex	9.6 ± 0.2	1.2 ± 0.4
2B5 MAb–cytochrome *c* complex	10.2 ± 0.04	1.6 ± 0.3

[a] Parameters are obtained from nonlinear least-squares fits of the pH dependence of the absorbance changes presented in Figure 8 to the equation $A = [A_H + A_L 10^{-n(pH-pK_{app})}]/[1 + 10^{-n(pH-pK_{app})}]$ where *A* is the absorbance of the equilibrium mixture of alkaline and native forms, A_H the absorbance of the alkaline form, A_L the absorbance of the native protein, and *n* the number of protons lost in the native to alkaline conformational change.

differing by a factor of 4-fold (3×10^{-5} s^{-1} vs 12×10^{-5} s^{-1}). The average of these values is listed in Table I. Estimates of the equilibrium binding constants calculated from the ratio of association and dissociation rate constants are given in Table I, assuming a two-state mechanism for the antibody–cytochrome *c* association reactions.

MAb–Cytochrome c Complex Formation and Shifts in the Equilibrium pK_{app} for the Alkaline Conformational Change. Optical spectroscopy shows that MAb binding at neutral pH leaves cytochrome *c* in a largely native conformation. Thus, as expected, both the 2B5 MAb and the 5F8 MAb, which were raised against native cytochrome *c*, prefer to bind to native epitopes. A preference for binding to native rather than alkaline cytochrome *c* requires that complex formation shift the pK_{app} for the alkaline conformational change to higher pH. Figure 8 shows that the expected shift in pK_{app} is observed. The pK_{app} is 9.3 for free cytochrome *c* while pK_{app} = 9.6 in the presence of MAb 5F8 and pK_{app} = 10.2 in the presence of MAb 2B5. Titration to the alkaline conformation involves loss of one proton for free cytochrome *c* and for the 5F8 MAb–cytochrome *c* complex (n = 0.8 ± 0.2 and n = 1.2 ± 0.4, respectively) but may involve an additional proton (n = 1.6 ± 0.3) for the 2B5 MAb–cytochrome *c* complex (Table III). For both MAbs, fluorescence measurements indicate that the complex remains intact over most of the pH range (pH 7–11) used to measure complex-induced shifts in pK_{app}. Thus, the shifts in pK_{app} represent an intramolecular stabilization which is expected to be largely independent of MAb concentration.

MAb Binding and the Rate of the Alkaline to Native Conformational Change. In Figure 9, the effect of MAb-

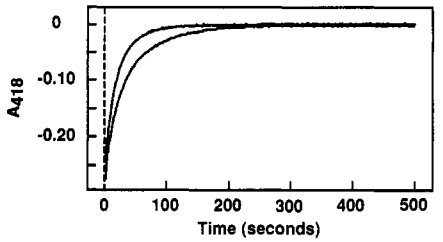

FIGURE 9: Comparison of the rate of the alkaline–native conformational change for free cytochrome *c* with that for the 2B5 MAb–cytochrome *c* complex. A large Soret band absorbance change characteristic of the alkaline conformational change allows the pH-induced reaction to be monitored by the absorbance at 418 nm for the MAb–cytochrome *c* complex (lower trace) and for free cytochrome *c* (upper trace). The alkaline–native conformational change was induced by manual mixing of cytochrome *c* initially at pH 10.0 in H_2O with 0.1 M sodium phosphate buffer to give a final pH = 7 at 20 °C. To achieve better base-line stability, the absorbance was monitored as the difference in absorbance at 418 and 800 nm. Absorbance changes at 800 nm are negligible for the alkaline conformational change and provide a measure of fluctuations in the instrument base line. Final protein concentrations are cytochrome *c* = 4×10^{-6} M and MAb = 2.0×10^{-6} M (4.0×10^{-6} M antigen binding sites).

alkaline cytochrome *c* complex formation on the rate of the alkaline to native conformational change is shown for MAb 2B5. 2B5 MAb–cytochrome *c* complex formation slows the alkaline–native conformational reaction slightly but signficantly (k_{obs} = 0.033 ± 0.008 s^{-1} for free cytochrome *c*, k_{obs} = 0.017 ± 0.005 s^{-1} for the 2B5 MAb–cytochrome *c* complex). This represents an additional activation free energy barrier of 0.46 kcal/mol for the alkaline conformational change within the 2B5 MAb–cytochrome *c* complex. Interestingly, 2B5 antibody increases the magnitude of the kinetically observed absorbance change at 418 nm by a factor of 1.17 relative to that of the alkaline conformational change for free cytochrome *c*. Similar results were obtained when monitoring this transition at a wavelength on the blue side of the Soret band (396 nm) where the absorbance changes have opposite sign. At 396 nm, the amplitude of the kinetic change in the presence of MAb 2B5 is 0.77 of that observed for free cytochrome *c*. This is consistent with the finding that the major Soret absorbance band for native cytochrome *c* increases slightly in intensity on forming a complex with antibody 2B5 (Figure 1). Experiments with MAb 5F8 show that there is no significant effect of 5F8 MAb–cytochrome *c* complex formation on the rate of the alkaline–native conformational change or on the amplitude of the kinetic changes monitored at 418 or 396 nm (data not shown).

DISCUSSION

Thermodynamic Reaction Rate Parameters for Antibody–Cytochrome c Binding. Diffusion-limited reactions are characterized by low activation enthalpies ($\Delta H^{\ddagger} \sim$ 3–4 kcal mol^{-1}) and by having an inverse dependence on solution viscosity (Amdur & Hammes, 1966). $\Delta H^{\ddagger}$ for 2B5 MAb–cytochrome *c* association ($\Delta H^{\ddagger}$ = 5.5 ± 0.1 kcal mol^{-1}) is slightly higher than that of a simple diffusion-controlled reaction. A plausible explanation is that diffusion-controlled reactions involving molecules of nonspherical geometry will include an activation energy term arising from orientational factors (Hill, 1975). In addition, correction of the observed $\Delta H^{\ddagger}$ for the effects of temperature on solvent viscosity lowers

$\Delta H^{\ddagger}$ into the range expected for diffusion-controlled association.[2]

Protein–protein interactions in general exhibit mostly positive values for $\Delta S^{\ddagger}$ which may result from charge neutralization and release of water molecules from within the binding site (Jencks, 1975). In contrast, the negative value of the activation entropy for the association reactions ($\Delta S^{\ddagger} = -12.8 \pm 0.4$ cal K^{-1} mol^{-1} for MAb 2B5 and $\Delta S^{\ddagger} = -17.6 \pm 2.7$ cal K^{-1} mol^{-1} for MAb 5F8) reflects additional order and increased polarity in the transition state, together with entropy losses in bringing the reactants together. Also, a charged group on either cytochrome *c* or the antibody which is not neutralized on complex formation can lead to an increase in the electrostriction and hence a negative $\Delta S^{\ddagger}$. The negative $\Delta S^{\ddagger}$ may derive from ordering of water molecules at the binding interface or especially stringent geometric factors in bringing the reactants together. Antibody combining sites have depth (~10 Å) (Hsia & Piette, 1969), and if cytochrome *c* binding traps water molecules in the cleft, association could lead to a decrease in $\Delta S^{\ddagger}$ (Jencks, 1975). The present state of transition-state theory does not allow for a more quantitiative interpretation of the $\Delta S^{\ddagger}$ values obtained.

Estimation of the Association Rate Constant for the MAb–Cytochrome c Binding Reaction. The measured second-order rate constants can be compared with the upper limit for a bimolecular association rate constant calculated from the Smoluchowski–Kollins–Kimball formalism (Berg & von Hippel, 1985). Using parameters appropriate for an antibody–protein antigen association reaction, a diffusion-limited association rate constant of 5×10^7 M^{-1} s^{-1} can be estimated. This is 35–100-fold larger than the experimentally determined rate constant (Table I). The factors that contribute to the observed difference could be orientational (Schmitz & Schurr, 1972), electrostatic (Eigen, 1964), or diffusive entrapment (Northrup & Erickson, 1992). A Brownian dynamics computer simulation of the kinetics of protein–protein association predicts rate constants in good agreement with those obtained for MAb–cytochrome *c* binding (Northup & Erickson, 1992). The observed rate constants for antibody–cytochrome *c* association fall within the range of values measured for other bimolecular protein–protein interactions (Koren & Hammes, 1976).

Differences in the rate of binding of an antibody to free cytochrome *c* versus an antibody–cytochrome *c* complex can also be estimated. Assuming all the other parameters remain constant and only the diffusion coefficients of the interacting species change, there should be a decrease in the rate constant by a factor of about $^1/_2$ for association between the 2B5 antibody and the 5F8 antibody–cytochrome *c* complex compared to the rate constant for association between the 2B5 antibody and cytochrome *c* alone. The values obtained (Table II) show a reduction in the rate constant by a factor of about 0.8 which is somewhat less than expected.

Viscosity Dependence of the Association Rate Constant Is Consistent with Diffusion Control. The extent to which a reaction is diffusion-limited has traditionally been studied by varying the viscosity of the medium with chemically inert co-solutes. A relative bimolecular rate ratio can be defined as k^0_1/k_1, where k^0_1 is the rate constant in buffer under standard conditions (no viscous agents) and k_1 is the rate constant in the presence of viscous agents. The relative bimolecular rate ratio, k^0_1/k_1 will be linearly dependent on the relative viscosity of the medium:

$$k^0_1/k_1 = A + B(\eta/\eta_0)$$

where A and B are constants. For an ideal diffusion-controlled reaction, $A = 0$ and $B = 1$ (Kramers, 1940). Values for B of less than 1.0 are interpreted as representing the fraction of diffusion control.

A potential problem is that the co-solute may induce a conformational change in the protein giving rate changes not related to solvent viscosity. For antibody 2B5, the extent to which the viscous additive alters chemical aspects of the rate has been tested by studying the viscosity dependence in the presence of both sucrose and glycerol (Figure 6). When sucrose was used as the viscous additive, a slope of 1.06 was obtained, consistent with essentially 100% diffusion-limited binding. In the presence of gycerol, a slope of 0.8 is obtained, corresponding to about 80% diffusion control. The results are consistent with the reaction being diffusion-controlled but also indicate a small chemical effect of one or the other viscous additives. For antibody 5F8, rate data have been obtained in the presence of sucrose alone. The slope is 1.2, indicating a diffusion-controlled reaction.

Ionic Strength Dependence of the Association Rate Constant. The ionic strength dependence of the bimolecular rate constant (Figure 7) is plotted according to the classical Debye–Hückel relationship:

$$\log k_1 = \log k^0_1 + Z_c Z_{Ab} I^{1/2}$$

where k_1 is the apparent second-order rate constant measured at ionic strength I, k^0_1 is the value of k_1 obtained by extrapolation to zero ionic strength, and Z_c and Z_{Ab} are charges on cytochrome *c* and the antibody, respectively.

For MAb 2B5–oxidized cytochrome *c* association, a linear dependence is observed with slope = –1.6 and an extrapolated value at zero ionic strength of $k^0_1 = 1.6 \times 10^6$ M^{-1} s^{-1} (at 5.6 °C). For MAb 2B5–reduced cytochrome *c* association, the slope is –1.7 and $k^0_1 = 1.4 \times 10^6$ M^{-1} s^{-1}. For both the oxidized and the reduced conformations, this corresponds to about a 4-fold increase in k_1 in going from an ionic strength of 0.14 to 0 M. Surprisingly, the slopes which in theory measure $Z_c Z_{Ab}$ are essentially the same for the oxidized and reduced protein, despite the fact that the formal charge on the heme iron atom differs by 1 for the two redox states. Classical Debye–Hückel theory which assumes Coulombic interactions between two spheres with charges uniformly distributed on their surface is a poor model for proteins such as cytochrome *c*. Therefore, the value of $Z_c Z_{Ab}$ (e.g., the slope) is best viewed as an empirical constant having uncertain physical significance.

The bimolecular rate constant for 2B5 antibody–cytochrome *c* association increases with decreasing ionic strength, as expected for a reaction between oppositely charged proteins. At pH 7.0, cytochrome *c* has a net positive charge (pI = 10), and isoelectric focusing studies on the antibodies used in this study show that they have a net negative charge, consistent with the ionic strength dependence of the rate constant.

The association rate has also been measured in 1 M salt to obtain a value for the binding rate constant under conditions where the charges on the macromolecules are essentially fully

[2] Aqueous bimolecular reactions with rates near the diffusion-controlled limit are strongly influenced by the viscosity of the medium in which the reaction occurs. For example, we have shown (Figure 6) that the association rate constant is inversely proportional to the solution viscosity ($k_1 \propto 1/\eta$) for the reaction between the 2B5 antibody and cytochrome *c*. Since solvent viscosity is temperature-dependent, the interpretation of temperature-dependent kinetics must also take into account temperature-induced changes in the solution viscosity (Gavish & Werber, 1979). If we correct the activation enthalpy obtained from the transition-state theory for the effect of temperature on solvent viscosity, the chemical component of the activation enthalpy for the reaction is 1.6 kcal/mol.

shielded. In going from 0.1 to 1 M salt, there is about a 2-fold decrease in the bimolecular rate constant for the 2B5 antibody–cytochrome *c* association for binding to both oxidized and reduced forms of the protein. This indicates that Coulombic interactions play only a minor role in this case. Thus, it appears that the contribution from charge–charge interactions to the binding rate is small.

Complex Formation Stabilizes the Native Conformation of Cytochrome c. At equilibrium, both antibodies preferentially stabilize the (oxidized) native conformation of cytochrome *c*, as would be expected of antibodies raised against the native protein. Antibody 2B5 had the largest effect on the pK_{app} for the transition from the native protein to the alkaline form. The pK_{app} for the complex with MAb 2B5 is 0.9 pH units higher (pK_{app} = 10.2) than in the absence of antibody (pK_{app} = 9.3). The complex with MAb 5F8 gives a more modest increase in pK_{app} (pK_{app} = 9.6) (Table III). Thus, complex formation increases the free energy of stabilization of the native over the alkaline form by 1.2 and 0.4 kcal/mol, respectively.[3]

Fluorescence measurements indicate that at the protein concentrations used for pH titrations of MAb–cytochrome *c* complexes, the complex remains largely intact as the protein antigen changes to the alkaline conformation. Nevertheless, there is a preference for binding to native cytochrome *c* (Figure 8). This suggests a degree of conformational adaptability within the MAb–protein antigen combining sites in order to accommodate the altered structures of the alkaline epitopes. This adaptability is not surprising in view of the well-known ability of an MAb to cross-react with closely related protein antigens.

Association Rate Constants Distinguish between Oxidized, Reduced, and Alkaline Conformers. The bimolecular rate constants for antibody binding to the oxidized-native, reduced-native, and alkaline forms depend weakly on the conformation of the protein antigen for MAb 2B5 but are independent of the cytochrome *c* conformation for MAb 5F8 (Table I). This may indicate small differences in the geometric or electrostatic components of the association rate constants for binding the 2B5 epitope (near residue 44) within different forms of cytochrome *c*. For binding to the oxidized or reduced forms, the ionic strength dependence is essentially the same, suggesting that the small difference in k_1 is attributable to the geometric factor. This is at least partially consistent with 2D NMR studies which show that residues 39–43 and 50–60 are involved in the redox-induced change in structure (Feng et al., 1990). These peptide chain segments almost certainly make up parts of the 2B5 MAb and 5F8 MAb binding epitopes, respectively.

MAbs as Tools for Characterizing Transition States for Protein Conformational Changes. Antibody 2B5 had a small but interesting effect on the kinetics of the transition from alkaline to native cytochrome *c*. When complexed to alkaline cytochrome *c*, this antibody slows the rate of the alkaline–native conformational change (Figure 9). This indicates that the 2B5 epitope on the alkaline cytochrome *c* molecule undergoes a structural rearrangement prior to the alkaline–native transition state. By binding alkaline cytochrome *c*, the antibody may decrease the flexibility of this region, making the conformational change needed to attain the transition state more difficult (by about 0.46 kcal/mol). The fact that antibody 5F8 does not affect the rate of the alkaline transition signficantly indicates that the region of the alkaline protein (near residue 60) bound by this antibody may have the same conformation in the alkaline form and the alkaline–native transition state.

Spectroscopic Analysis of Antibody–Cytochrome c Complexes. Changes in the absorbance spectrum of cytochrome *c* similar to those found for the 2B5 antibody–cytochrome *c* complex have been reported for the reactions of cytochrome *c* with cytochrome b_5, cytochrome *c* peroxidase, and cytochrome oxidase (Erman & Vitello, 1980; Mauk et al., 1982; Michel et al., 1989). Such changes in the absorbance spectrum can be qualitatively interpreted as a decrease in the dielectric constant in the vicinity of the exposed heme crevice on antibody binding. The red shift in the Soret maximum is in accord with the heme being less exposed in the complex than in native cytochrome *c* (Stellwagen, 1964).

CD spectra of the Soret region of the 2B5 antibody–cytochrome *c* complex show a rather large decrease in the intensity of the major Soret CD bands. While the spectral changes show that a change in heme environment has occurred, they do not necessarily prove that the CD changes result from a structural change in cytochrome *c*. The 2B5 antibody is known to bind in the vicinity of the heme crevice and might change the symmetry and polarity of the heme environment by proximity rather than by inducing a structural change. Nevertheless, an induced structural change of unknown proportions may well be the most likely explanation for the CD changes. The spectrum resulting from 2B5 binding to cytochrome *c* appears to be unique in that it is very different from that produced when cytochrome *c* interacts with electron-transfer proteins. For example, the interaction of cytochrome *c* with cytochrome oxidase, cytochrome *c* peroxidase, flavodoxin, and cytochrome c_1 results in an increase in the positive cotton effect near 405 nm along with loss of the band near 417 nm (Chiang et al., 1976; Michel et al., 1989; Saad & Bosshard, 1990; Tollin et al., 1987). Similar results have also been obtained with monoclonal antibody binding to *Rhodospirillium rubrum* cytochrome c_2 (Saad & Bosshard, 1990). These results have been interpreted as indicating a loosening of the heme crevice (Myer, 1985). Our results, in which the CD intensity changes are largely opposite in sign, suggest that formation of the 2B5 MAb–cytochrome *c* complex involves tightening of the heme crevice.

The CD spectrum of the 5F8 antibody–cytochrome *c* complex is essentially the same as that of free cytochrome *c*. This provides a useful negative control experiment that shows that high-affinity antibody binding can occur in the absence of changes in the Soret CD spectrum.

CONCLUSIONS

Measurements of the effects of temperature, viscosity, and ionic strength on bimolecular rate constants for antibody–cytochrome *c* association yield results that are consistent with a diffusion-controlled reaction mechanism. The magnitude of the rate constants, while comparable to those measured for other protein–protein association reactions, suggests stringent orientational requirements for binding. The rate constant decreases linearly as the square root of the ionic strength increases, in qualitative accord with expectations for a reaction between oppositely charged macromolecular species. For one MAb (2B5) but not the other (5F8), the association rate constant depends weakly on cytochrome *c* conformation. This likely reflects small changes in the geometric or electrostatic components of the diffusion-controlled association rate constant.

[3] We assume that $\Delta G^\circ = 2.303pK_{app}$ is the free energy change for forming the alkaline from the native conformation: $\Delta\Delta G^\circ = \Delta G^\circ$(complex $- \Delta G^\circ$(free) $= -2.303\ RT\Delta pK_{app}$, where $\Delta pK_{app} = pK_{app}$(complex) $- pK_{app}$(free).

Spectroscopic analysis of the complexes formed between the antibodies and cytochrome *c* shows that binding of one of the antibodies to cytochrome *c* perturbs the heme environment, suggesting the possibility of a binding-induced conformational change in the protein antigen.

ACKNOWLEDGMENT

The authors thank Scott H. Northrup, Robert L. Baldwin, and the reviewers for helpful suggestions and discussion.

REFERENCES

Amdur, I., & Hammes, G. G. (1966) *Chemical Kinetics, Principles and Selected Topics*, McGraw-Hill, New York.
Berg, O. G., & von Hippel, P. H. (1985) *Annu. Rev. Biophys. Biophys. Chem. 14*, 131–160.
Brautigan, D. L., Ferguson-Miller, S., & Margoliash, E. (1978) *Methods Enzymol. 53*, 128–164.
Bushnell, G. W., Louie, G. V., & Brayer, G. D. (1990) *J. Mol. Biol. 214*, 585–595.
Chiang, Y.-L., Kaminsky, L. S., & King, T. E. (1976) *J. Biol. Chem. 251*, 29–36.
Corradin, G., Juillerat, M. A., & Engers, H. D. (1984) *J. Immunol. 133*, 2915–2919.
Davis, L. A., Schejter, A., & Hess, G. P. (1974) *J. Biol. Chem. 249*, 2624–2632.
Dohne, S. M., Elove, G. A., Roder, H., & Nall, B. T. (1989) *Biophys. J. 55*, 557a.
Eden, D., Matthew, J. B., Rosa, J. J., & Richards, F. M. (1982) *Proc. Natl. Acad. Sci. U.S.A. 79*, 815–819.
Eigen, M. (1964) *Agnew. Chem., Int. Ed. Engl. 3*, 1–19.
Erman, J. E., & Vitello, L. B. (1980) *J. Biol. Chem. 255*, 6224–6227.
Feng, Y., Roder, H., & Englander, S. W. (1990) *Biochemistry 29*, 3494–3504.
Friguet, B., Chaffotte, A. F., Djavadi-Ohaniance, L., & Goldberg, M. (1985) *J. Immunol. Methods 77*, 305–319.
Friguet, B., Djavadi-Ohaniance, L., & Goldberg, M. (1989) *Res. Immunol. 140*, 355–376.
Gavish, B., & Werber, M. M. (1979) *Biochemistry 18*, 1269–1275.
Gelsema, W. L., De Ligny, C. L., & Van der Veen, N. G. (1977) *J. Chromatogr. 140*, 149–155.
Goshorn, S. C., Retzel, E., & Jemmerson, R. (1991) *J. Biol. Chem. 266*, 2134–2142.
Gupta, R. K., & Koenig, S. H. (1971) *Biochem. Biophys. Res. Commun. 45*, 1134–1143.
Hamilton, R. G., Roebber, M., Reimer, C. B., & Rodkey, L. S. (1987) *Electrophoresis 8*, 127–134.
Hennessey, J. P., & Johnson, W. C., Jr. (1982) *Anal. Biochem. 125*, 177–188.
Hettinger, T. P., & Harbury, H. A. (1964) *Proc. Natl. Acad. Sci. U.S.A. 52*, 1469–1476.
Hill, T. L. (1975) *Prod. Natl. Acad. Sci. U.S.A. 72*, 4918–4922.
Hsia, J. C., & Piette, L. H. (1969) *Arch. Biochem. Biophys. 129*, 296–307.
Jencks, W. P. (1975) *Adv. Enzymol. Relat. Areas Mol. Biol. 43*, 219–410.
Koren, R., & Hammes, G. G. (1976) *Biochemistry 15*, 1165–1171.
Kramers, H. A. (1940) *Physica (Amsterdam) 7*, 284–304.
Kranz, D. M., Herron, J. N., & Voss, E. W. J. (1982) *J. Biol. Chem. 257*, 6987–6995.
Margoliash, E., & Frohwirt, N. (1959) *Biochem. J. 71*, 570.
Mauk, M. R., Reid, L. S., & Mauk, A. G. (1982) *Biochemistry 21*, 1843–1846.
Michel, B., Proudfoot, A. E. I., Carmichael, J. A. W., & Bossard, H. R. (1989) *Biochemistry 28*, 456–462.
Myer, Y. P. (1985) *Curr. Top. Bioenerg. 14*, 149–188.
Noble, R. W., Reichlin, M., & Gibson, Q. H. (1969) *J. Biol. Chem. 244*, 2403–2411.
Northrup, S. H., & Erickson, H. P. (1992) *Proc. Natl. Acad. Sci. U.S.A. 89*, 3338–3342.
Robertson, E. F., Dannelly, H. K., Malloy, P. J., & Reeves, H. C. (1987) *Anal. Biochem. 167*, 290–294.
Saad, B., & Bosshard, H. R. (1990) *Eur. J. Biochem. 187*, 425–430.
Schmitz, K. S., & Schurr, J. M. (1972) *J. Phys. Chem. 76*, 534–548.
Shechter, E., & Saludjian, P. (1967) *Biopolymers 5*, 788–790.
Smith, H. T., & Millett, F. (1980) *Biochemistry 19*, 1117–1120.
Stellwagen, E. (1964) *Biochemistry 3*, 919.
Stevens, F. J. (1987) *Mol. Immunol. 24*, 1055–1060.
Takano, T., & Dickerson, R. E. (1981a) *J. Mol. Biol. 153*, 79–94.
Takano, T., & Dickerson, R. E. (1981b) *J. Mol. Biol. 153*, 95–115.
Tollin, G., Brown, K., Francesco, R. D., & Edmondson, D. E. (1987) *Biochemistry 26*, 5042–5048.
Wallace, C. J. (1984) *Biochem. J. 217*, 601–604.
Wand, A. J., Roder, H., & Englander, S. W. (1986) *Biochemistry 25*, 1107–1114.
Weast, R. C. (1984) *CRC Handbook of Chemistry and Physics*, CRC Press, Boca Raton, Fl.
Wilgus, H., & Stellwagen, E. (1974) *Proc. Natl. Acad. Sci. U.S.A. 71*, 2892–2894.

Registry No. Cytochrome *c*, 9007-43-6; heme, 14875-96-8.